Hindawi Publishing Corporation
Journal of Nanomaterials
Volume 2016, Article ID 6547271, 7 pages
http://dx.doi.org/10.1155/2016/6547271

Research Article

Effect of HCl on the Formation of TiO_2 Nanocrystallites

Nguyen Trong Tung[1,2] and Duong Ngoc Huyen[1]

[1]*School of Engineering Physics, Hanoi University of Science and Technology, No. 1 Daicoviet, Hanoi 112400, Vietnam*
[2]*College of Television Vietnam, Thuong Tin, Hanoi 158500, Vietnam*

Correspondence should be addressed to Duong Ngoc Huyen; huyen.duongngoc@hust.edu.vn

Received 29 August 2016; Revised 9 November 2016; Accepted 1 December 2016

Academic Editor: Jim Low

TiO_2 nanocrystals are prepared by pyrolysis of titanium tetrachloride ($TiCl_4$) as precursor in HCl aqueous solution at 80°C. The experimental results show that the HCl concentrations in the synthesizing medium and the following aging are the essential factors affecting the phase formation and phase composition of the resulting TiO_2 nanocrystals. The TiO_2 suspended in the HCl media is predominant anatase in uniform cluster and the TiO_2 deposited in the sedimentation is predominant rutile in the rod-like structure. In the anatase phase, TiO_2 crystallites have particle structure of 4–11 nm in mean size depending on the HCl concentration and aging time. In the rutile phase, the mean size of rutile TiO_2 is 12-13 nm and there is not much change with HCl environment and aging time. The mean size of TiO_2 of around 11-12 nm is considered to be the critical point of phase transition from anatase to rutile in HCl media. Consequence, TiO_2 nanocrystallites in pure anatase and rutile phase can be extracted and segregated from the colloidal suspension and the deposited parts in the synthesizing media.

1. Introduction

Titanium dioxide (TiO_2), a typical oxide metal and *n*-type semiconductor, exhibits strong photoactivity involving photogenerated charge carrier reaction of adsorbed substances and photoinduced hydrophilic conversion of itself. Being a safe material with high refractive index, chemical stability, long durability, nontoxicity, and low cost, TiO_2 has found a great potential for wide applications in pigments, catalyst supports, ultraviolet fillers, coatings, photoconductor, photocatalyst, environment cleaning, chemical sensors, and so forth [1–4]. For example, photochemical activities of TiO_2 are widely utilized for antibacterial purpose, self-cleaning glass, and water purification [2]. The ultraviolet absorbance of TiO_2 nanoparticles is used to filter the sunlight and is used in cosmetics to protect the skin [5]. With respect to photoelectrical features, TiO_2 is used to convert light into electricity in dye-sensitized solar cells (DSSC) or to separate hydrogen from water for fuel cells [5, 6].

Under normal condition, TiO_2 exists in three main structures: stable rutile, metastable anatase, and brookite; this later polymorph is difficult to synthesize and characterize so that it is almost ignored in this study. Despite the larger band gap of anatase of ~3.2 eV in comparison to ~3.0 eV of rutile, the photocatalytic activity of anatase is commonly considered superior to that of rutile. This is attributed to a higher density of localized states and slower charge carrier recombination in anatase relative to rutile [7]. On the other hand, some studies made on high-area rutile of acicular morphology or phase mixture have suggested that rutile may be advantageous for certain applications [8–10]. Furthermore, TiO_2 nanostructure can be crystallized in the form of nanotubes, nanowires, nanorods, and nanoparticles [6, 7, 11–13]. The difference in morphology, crystal, and electronic structure of TiO_2 polymorphs results in difference in overall photoactivities and potential applications. Therefore, an understanding of the formation of TiO_2 polymorphs, their transition, and the mechanism by which the desirable polymorph can be achieved is critical to have an optimal photocatalytic performance.

For the preparation of TiO_2 nanostructure, a variety of synthesis methods such as hydrothermal, solvothermal, sol-gel, direct oxidation, chemical vapor deposition (CVD), electrodeposition, sonochemical, and microwave method has

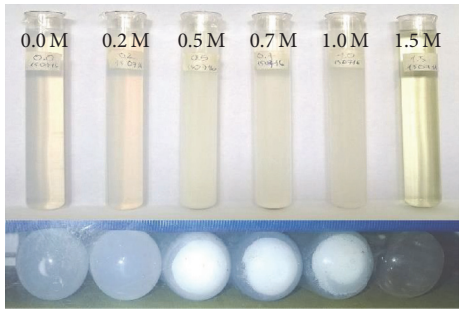

Figure 1: The suspension and deposited TiO_2 by pyrolysis of $TiCl_4$ in different HCl aqueous solution.

been used [6, 7, 13]. Hydrothermal method offers a simple and common route to synthesize a well-crystalline TiO_2 under the moderate reaction condition such as low temperature and short time using inexpensive precursors such as $TiCl_4$, $TiCl_3$, amorphous TiO_2, and P25 [14–18]. In addition, hydrothermal media provide an effective reaction environment for the nucleation and growth of TiO_2 nanostructure with high purity, good dispersion, and controllable crystalline. The synthesis conditions such as temperature, pH, and time are considered as the critical parameters to control and achieve the desirable TiO_2 nanostructures including size, morphology, and phase composition [19, 20]. For the $TiCl_4$ precursor, the presence of HCl in the hydrothermal medium has been shown to strongly affect the crystalline phase formation of TiO_2 nanostructures [12, 19, 21]. In this study, pyrolysis of $TiCl_4$ at relative low temperature of 80°C in HCl aqueous solution is used to study the formation of TiO_2 polymorphs. The effect of HCl and aging time on the TiO_2 formation and anatase to rutile phase transition is presented and discussed.

2. Experiment

Titanium tetrachloride ($TiCl_4$) of 99.9% purity (Sigma Aldrich Chemical Co.) and HCl 37% solution (Merck Corp.,) were used as received. The TiO_2 synthesis process is straightforward as follows: a $TiCl_4$ aqueous solution with a fixed concentration of 0.4 M and HCl ranging from 0.0 to 1.5 M was used as starting materials. This solution then was poured into test tubes and placed in an oven at 80°C. The solution was gradually changed to opaque suspension indicating that the $TiCl_4$ was thermally decomposed and segregated into TiO_2 in the reaction medium. After 3.0 h heating, the solution was cooled to room temperature and some white powder was separated and deposited on the bottom of the test tubes as clearly seen in Figure 1. The upper suspension solution and bottom sedimentation part contains the colloid and deposited TiO_2 with different size and phase composition. The test tubes then were kept at room temperature for months to study the aging effect. After a known period of aging time, the resulting TiO_2 from the colloidal solution and sedimentation part was extracted and dried by vacuum evaporation, rinsed with distilled water, and analyzed for crystalline structure.

The structures of the TiO_2 were determined using XRD, Raman spectra, and TEM with high resolution. XRD experiments were carried out in a D8 Advance Bruker diffractometer using CuK_α radiation, $\lambda = 0.154056$ nm. The mean size D of resulting TiO_2 is calculated using Scherrer formula:

$$D = \frac{k\lambda}{\beta \cos\theta}, \tag{1}$$

where $k = 0.94$, $\lambda = 0.154056$ nm is X-ray wavelength (CuK_α), and β is full width at half maximum (FWHM) (rad.) according to diffracted angle θ, that is, at (110) peak for rutile and (101) peak for anatase. Phase composition of anatase W_A and rutile W_R was calculated by comparing the XRD intensity of (110) peak and (101) peak for rutile and anatase, respectively, as the following formulas (Spurr and Myers):

$$W_A = \frac{1}{1 + 1.26\left(I_R/I_A\right)}, \qquad W_R = \frac{1}{1 + 0.8\left(I_A/I_R\right)}, \tag{2}$$

where W_A and W_R are the weight fraction of anatase and rutile in the resulting TiO_2; I_A and I_R are the XRD intensity of (110) and (101) peak for rutile and anatase, respectively.

Raman spectra were carried out in LabRAM HR800 (Horiba) using a 632.8 nm excitation laser at a resolution of 1.0 cm^{-1}. The morphology and particle size were determined using a JEOL JEM-2100 Transmission Electron Microscopy (HRTEM).

3. Results and Discussion

X-ray diffraction and Raman spectra show that the resulting TiO_2 exists in both phases, namely, anatase and rutile phase. The anatase and rutile weight ratio (phase composition) in the suspension solution and sedimentation parts are different depending on the HCl concentration and the aged time.

Right after the pyrolysis, the XRD made on the TiO_2 extracted from the suspension solution indicates most the principal diffraction peaks belong to anatase. As can be seen from Figure 2, the strongest peak observed around 25.29° is assigned to (101) plane refraction of anatase and also the other peaks at 37.80, 48.05, 53.89, and 62.68° stand for reflection at (004), (200), (105), and (204) planes, respectively. From XRD powder diffraction patterns of anatase (JCPDS number 00-021-1272), the intensities of (004) and (200) relatively increase incomparison to that of (101) peak with increasing HCl concentration. The feature indicates an increase in anatase size growth preferably along (101) and (004) direction. In the XRD patterns, a small trace of rutile is also observed. Using Scherrer formula to estimate the mean size it was found that at 0.0 M HCl the anatase size is around 4.0 nm and grows to 9.0 nm at 1.0 M HCl. With increase in aging time, the suspension solution in the test tube becomes more transparent as a result of deposition. However, dried in vacuum a purer TiO_2 anatase is gained from the solution. The XRD in Figure 3 shows that principal diffraction peaks standing for anatase phase are clearer and sharper while

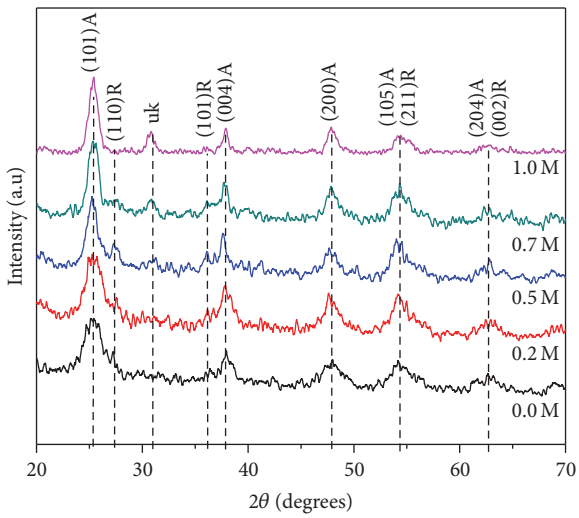

Figure 2: XRD patterns of initial TiO_2 in suspension solution.

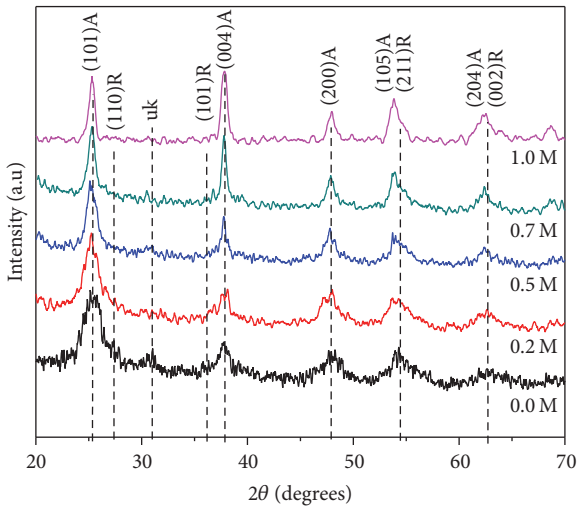

Figure 3: XRD patterns of aged TiO_2 in suspension solution.

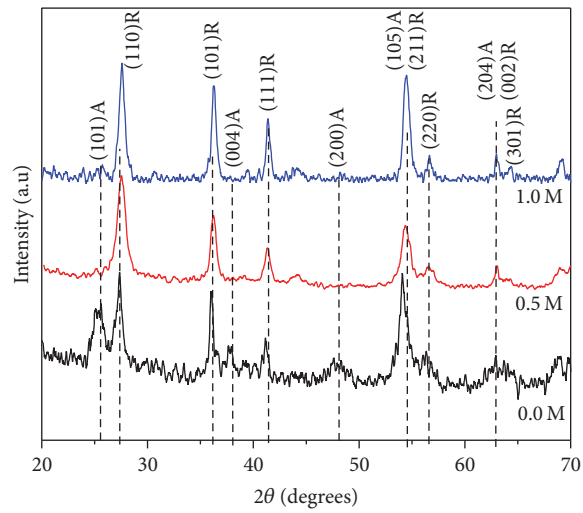

Figure 4: XRD patterns of initial TiO_2 deposited in sedimentation part.

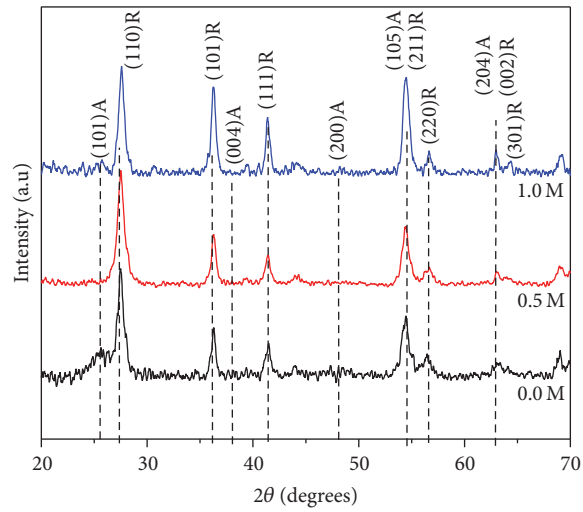

Figure 5: XRD patterns of aged TiO_2 deposited in sedimentation part.

those standing for rutile phases disappeared. Similar to those of initial TiO_2, an increase in anatase size with HCl concentration is observed. The mean size of anatase is around 5 nm in 0.0 M HCl sample and increases to 11 nm in 1.0 M HCl sample.

On the other hand, the resulting TiO_2 in the sedimentation at the bottom of the test tube exhibits the other trend. The XRD patterns show that the deposited TiO_2 is predominant rutile. As shown in Figures 4 and 5, the positions of all intense diffraction peaks correspond to rutile; namely, the strongest peak observed at 2θ of 27.37° is assigned to (110) plane refraction and the other peaks observed at 2θ of 36.10°, 41.26°, 54.36°, 56.59°, 62.92°, and 68.91° stand for the refraction at (101), (111), (211), (220), (002), and (301) planes, respectively (JCP2.2CA number 00-021-1276). The intensity of the (101) peak is relatively heightened and its FWHM is shrunk. The feature indicates that the resulting TiO_2 rutile crystallites are major nanorods growth preferably in [001] direction and the (101) planes are the sidewall of TiO_2 nanorods which are preferentially exposed to X-ray [22, 23].

Experiment result shows that the relative rutile fraction in the sedimentation part increases with the HCl concentration and aging time. As shown by XRD patterns in Figure 4, the initial TiO_2 deposited in sedimentation part is a mixture of anatase and rutile phase with predominant rutile. In 0.0 M HCl medium, some of principal diffraction peaks standing for anatase such as (110) and (200) are observed but disappear at higher HCl concentration, say at 0.5 M and 1.0 M HCl. In aged sample, the XRD spectra show that the relative anatase fraction in the sedimentation part is reduced and the relative rutile fraction is increased (Figure 5). The mean particle size of rutile particles is around 12–13.0 nm for all sample while that of anatase is 6-7 nm. Comparing the XRD patterns made on the initial and aged TiO_2 deposited in the same

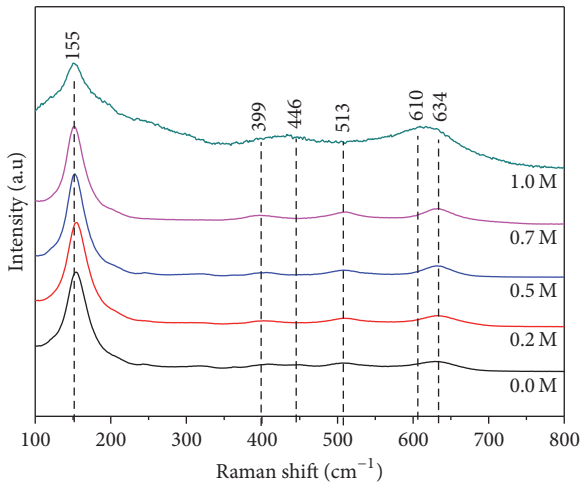

Figure 6: Raman spectra of initial TiO_2 in suspension solution.

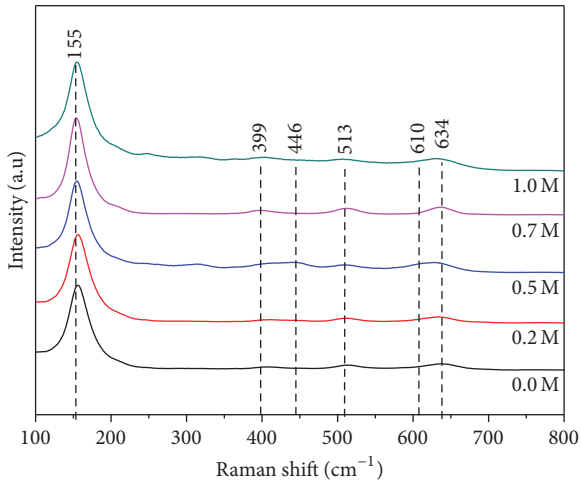

Figure 7: Raman spectra of aged TiO_2 in suspension solution.

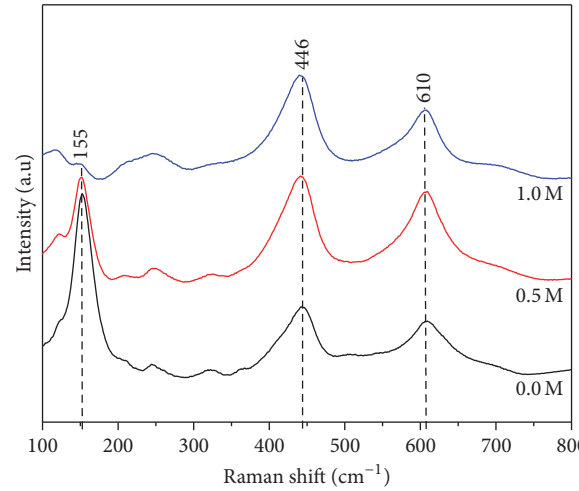

Figure 8: Raman spectra of initial TiO_2 deposited in sedimentation part.

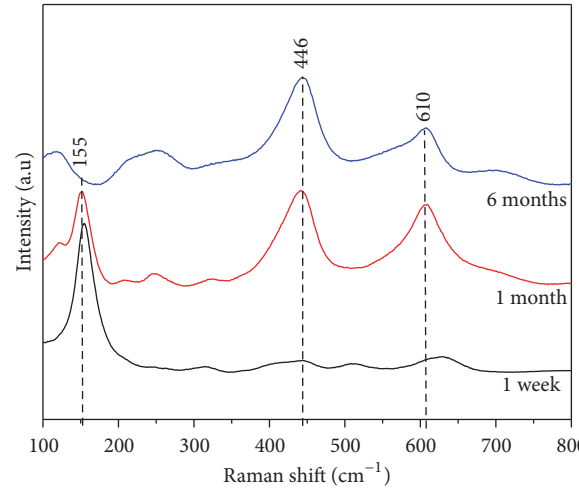

Figure 9: Raman spectra of aged TiO_2 deposited in 0.5 M HCl.

HCl medium (Figures 2–5), it can be deduced that the TiO_2 undergoes a phase transition from anatase to rutile occurring at a critical size round 11-12 nm [7, 24]. HCl medium and aging time are factors affecting the anatase to rutile phase transition. A pure rutile phase in nanorod form growth in [001] direction can be achieved at HCl acidic aqueous solution in a long time aging.

The Raman spectra also add more evidence to confirm the phase transition process and reveal the properties of TiO_2 crystallites in the suspension solution and sedimentation part. The Raman spectra of the suspended TiO_2 exhibit vibrational modes at around 155, 399, 513, and 634 cm^{-1} (Figures 6 and 7) representing the E_g, B_{1g}, A_{1g} + B_{1g}, and E_g modes of anatase phase, respectively [14]. In comparison to the standard vibration mode of anatase, the first E_g mode at 155 cm^{-1} shows blue shifts in frequency and increase in width at half maximum that accounts for an influence of the nanosize of the TiO_2 crystallites. The Raman spectrum of TiO_2 aging in HCl 0.5 M shows the appearance of vibration mode at 466 cm^{-1} representing the rutile phase [14]. After aging in the HCl acidic aqueous solution, the FWHM of the vibrational E_g modes decreases (Figure 7) indicating an increase in size of anatase TiO_2 particles. The intensity of vibrational mode of the pattern in 1.0 M HCl is greater than that in the 0.0 M HCl solution.

On the other hand, the Raman analysis made on resulting TiO_2 deposited in the sedimentation part also provides the evidence of the phase transition. The shift of vibration modes standing for anatase to those of rutile in Raman spectra as can be seen in Figure 8 and Figure 9 indicates the transition from anatase to rutile with HCl concentration and aging time. For example, a clear reduction in intensity of anatase vibration mode at 155 cm^{-1} and an increase in that of rutile at 610 cm^{-1} peak is observed in the TiO_2 deposited in 0.0 M, 0.5 M, and 1.0 M HCl, respectively. With respect to aging time, a similar behavior is observed for the TiO_2 deposited in 0.5 M HCl (Figure 9). Pure rutile phase can be seen in the initial 1.0 M

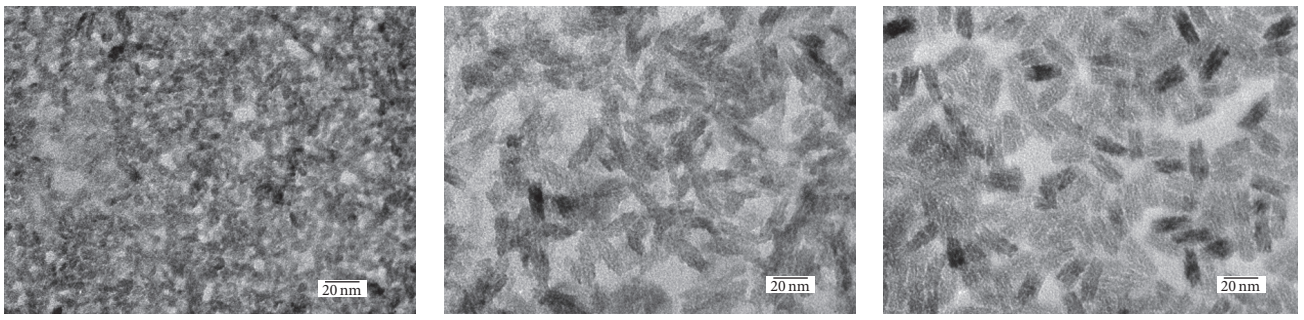

(a) (b) (c)

Figure 10: TEM images of initial TiO_2 in suspension solution of (a) 0.0 M, (b) 0.5 M, and (c) 1.0 M HCl.

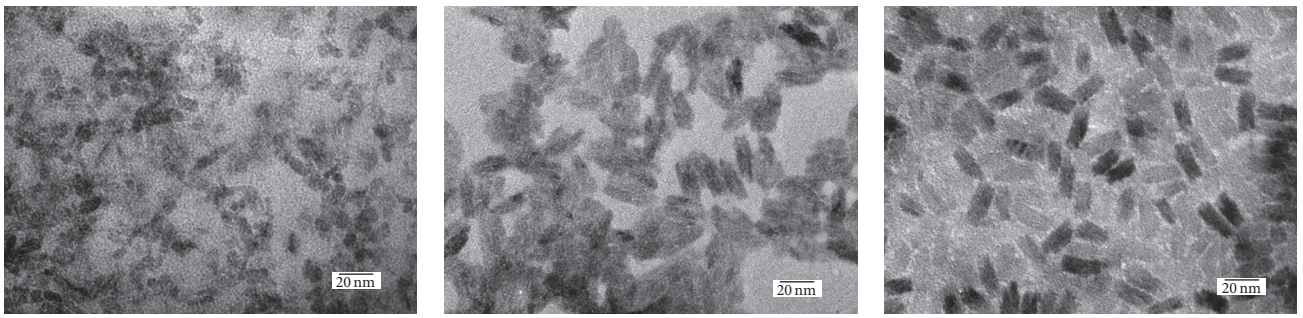

(a) (b) (c)

Figure 11: TEM image of aged TiO_2 in suspension solution of (a) 0.0 M, (b) 0.5 M, and (c) 1.0 M HCl.

HCl sample and aged 0.5 M HCl sample is the same as the results in XRD measurements.

From XRD and Raman study, it can be briefly concluded that with aging time the anatase phase content in the suspension solution increases as a result of coupling of small anatase crystallites and growing process while the rutile phase content in the sedimentation gradually increases due to the phase transition from anatase to rutile. During the growth of TiO_2, the presence of HCl prevents TiO_2 rutile from increasing activation energy. Thus, the anatase TiO_2 in HCl can grow larger. In higher concentration HCl solution: Cl^{-1} may affect the bonding structure of TiO_2 and is likely to form rutile nanorods. The enhancement of the rutile phase growth and phase transition in this experiment is attributed to the HCl-rich environment [12, 17, 19].

As a complementary, the TiO_2 morphology in the suspension and sedimentation part observed through TEM images provides a light on the tendency of TiO_2 transition. From XRD and Raman measurements, TiO_2 in suspension is predominant anatase phase and the TiO_2 in the sedimentation is the predominant rutile phase. As can be seen from Figures 10 and 11, the TiO_2 crystallites in the suspension solution form uniform grain-like cluster and the cluster size increases with HCl concentration. At 0.0 M HCl, the TiO_2 grain size is smaller around 4-5 nm which is the same size as calculation from XRD pattern. However, depending on HCl and aging time the TiO_2 grain size can reach a uniform size of around 20 nm. In comparison to that of anatase particle (4 nm–11 nm) as calculated from XRD, it can be deduced that the suspended TiO_2 grain is a cluster of many smaller anatase particles.

The initial and aged TiO_2 deposited in the sedimentation is a mixture of anatase and rutile phase whose morphology is shown in Figures 12 and 13. At the early stage, many particles with the size of 20–30 nm (rutile) are formed and agglomerated to form big clusters and extract small anatase particles on the surface of them. Rutile with higher mass density (4.23 in comparison to 3.78 of anatase) will have higher rate of deposition in HCl aqueous solution. With increasing time, the rutile will continue growth with anatase consumption and gradually precipitated as sedimentation with aging time at the bottom of test tubes. As a result, the portion of rutile is increased while that of the anatase is decreased.

Based on experiment results, the formation of TiO_2 nanostructures with different crystalline phases and morphology in HCl acidic aqueous medium is explained by two mechanisms: one is the dissolution and recrystallization and the other is the in situ transition [12]. The formation of anatase in suspension part is likely belonging to the first mechanism and the formation of rutile in the sedimentation is belonging to the second mechanism. The first mechanism governs the formation of anatase and is followed by the second mechanism as a correlation between the free energy

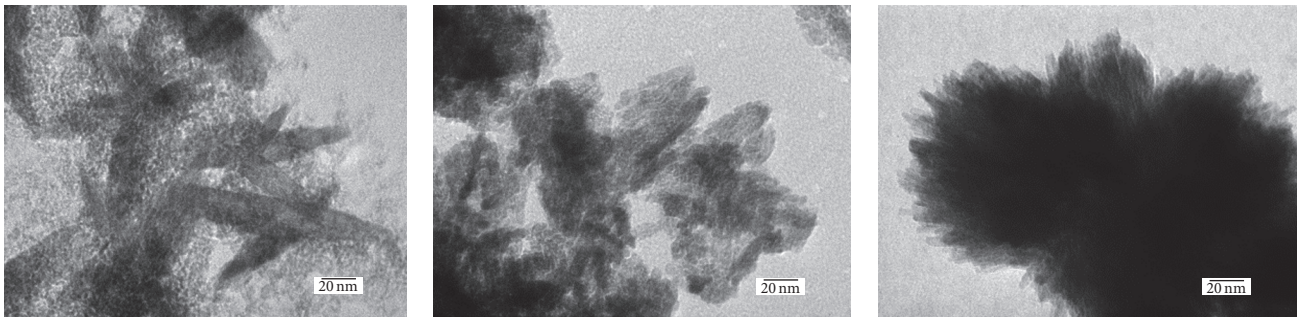

(a) (b) (c)

Figure 12: TEM images of initial TiO_2 deposited in sedimentation in acidic solution of (a) 0.0 M, (b) 0.5 M, and (c) 1 M HCl.

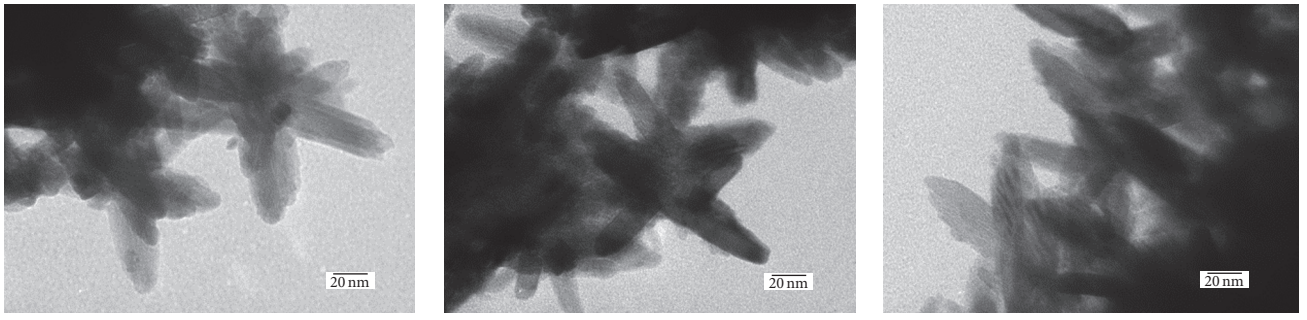

(a) (b) (c)

Figure 13: TEM image of aged TiO_2 deposited in sedimentation in acidic solution of (a) 0.0 M, (b) 0.5 M, and (c) 1.0 M HCl.

and the size limitation of TiO_2 colloids [7, 24, 25]. As a competition between the surface and bulk free energy, below a size limitation (9–11 nm), the TiO_2 rutile crystallites have higher free energy than that of the anatase and vice versa [24, 25]. Consequently, the resulting TiO_2 in the solution is predominant anatase phase as the size is below the limitation. As the size exceeds the limitation the in situ anatase to rutile transition occurs; rutile crystallites with bigger size are formed and then deposited in the sedimentation. In the equilibrium condition, the smaller particles in the colloidal solution are predominant anatase, and the bigger nanoparticle that will deposit at the bottom of the flask will be predominant rutile. The anatase to rutile transition is enhanced by the presence of HCl. A solvent environment with the presence of HCl creates Ti_4^+ ion converting solvent and the formation of TiO_2 crystals, which makes the split of crystals in the anatase and rutile phase easier. During the TiO_2 growth process, HCl worked like a chemical catalyst causing a change in crystallization and decreasing the activation energy for the rutile formation [12]. By adjusting the HCl concentration, the rutile/anatase ratio is changed as the equilibrium condition is changing.

4. Conclusion

TiO_2 nanocrystals synthesized by a pyrolysis of $TiCl_4$ in HCl acidic aqueous medium are found to be crystallized in two separate phase structures. The TiO_2 suspended in the HCl media is predominant anatase in uniform cluster while the TiO_2 deposited in the sedimentation is predominant rutile in the rod-like structure. In the anatase phase, TiO_2 crystallites have a particle structure 4–11 nm in size depending on the HCl concentration and aging time. In the rutile phase, the mean size of rutile TiO_2 is 12-13 nm and there is not much change with HCl environment and aging time. The HCl environment enables the agglomeration of small anatase particles forming uniform cluster and enhances the anatase to rutile transition. The mean size around 11-12 nm is considered to be the critical point of phase transition from anatase to rutile in HCl media. Pure anatase and rutile phase then can be extracted and separated by choosing a suitable HCl concentration and a proper aging time.

Competing Interests

The authors declare that they have no competing interests.

Acknowledgments

The authors gratefully acknowledge financial support received in the form of a Basic Research Project Grant in Aid (no. 103.02-2012.32) provided by the National Foundation for Science and Technology Development (NAFOSTED), Vietnam.

References

[1] A. Fujishima and K. Honda, "Electrochemical photolysis of water at a semiconductor electrode," *Nature*, vol. 238, no. 5358, pp. 37–38, 1972.

[2] K. Hashimoto, H. Irie, and A. Fujishima, "TiO_2 photocatalysis: a historical overview and future prospects," *Japanese Journal of Applied Physics*, vol. 44, no. 12, pp. 8269–8285, 2005.

[3] S. N. Frank and A. J. Bard, "Heterogeneous photocatalytic oxidation of cyanide ion in aqueous solutions at titanium dioxide powder," *Journal of the American Chemical Society*, vol. 99, no. 1, pp. 303–304, 1977.

[4] D. N. Huyen, N. T. Tung, N. D. Thien, and L. H. Thanh, "Effect of TiO_2 on the gas sensing features of TiO_2/PANi nanocomposites," *Sensors*, vol. 11, no. 2, pp. 1924–1931, 2011.

[5] K. Nakata and A. Fujishima, "TiO_2 photocatalysis: design and applications," *Journal of Photochemistry and Photobiology C: Photochemistry Reviews*, vol. 13, no. 3, pp. 169–189, 2012.

[6] S. M. Gupta and M. Tripathi, "A review of TiO_2 nanoparticles," *Chinese Science Bulletin*, vol. 56, no. 16, pp. 1639–1657, 2011.

[7] D. A. H. Hanaor and C. C. Sorrell, "Review of the anatase to rutile phase transformation," *Journal of Materials Science*, vol. 46, no. 4, pp. 855–874, 2011.

[8] T. T. Nguyen and N. H. Duong, "Effect of TiO_2 rutile additive on electrical properties of PPy/TiO_2 nanocomposite," *Journal of Nanomaterials*, vol. 2016, Article ID 4283696, 6 pages, 2016.

[9] T. Ohno, K. Tokieda, S. Higashida, and M. Matsumura, "Synergism between rutile and anatase TiO_2 particles in photocatalytic oxidation of naphthalene," *Applied Catalysis A: General*, vol. 244, no. 2, pp. 383–391, 2003.

[10] T. Ohno, K. Sarukawa, and M. Matsumura, "Crystal faces of rutile and anatase TiO_2 particles and their roles in photocatalytic reactions," *New Journal of Chemistry*, vol. 26, no. 9, pp. 1167–1170, 2002.

[11] Y. Lei, L. D. Zhang, and J. C. Fan, "Fabrication, characterization and Raman study of TiO_2 nanowire arrays prepared by anodic oxidative hydrolysis of $TiCl_3$," *Chemical Physics Letters*, vol. 338, no. 4–6, pp. 231–236, 2001.

[12] S. Dai, Y. Wu, T. Sakai, Z. Du, H. Sakai, and M. Abe, "Preparation of highly crystalline TiO_2 nanostructures by acid-assisted hydrothermal treatment of hexagonal-structured nanocrystalline titania/cetyltrimethyammonium bromide nanoskeleton," *Nanoscale Research Letters*, vol. 5, no. 11, pp. 1829–1835, 2010.

[13] M. M. Byranvand, A. Nemati Kharat, L. Fatholahi, and Z. Malekshahi Beiranvand, "A review on synthesis of nano-TiO_2 via different methods," *Journal of Nanostructures*, vol. 3, pp. 1–9, 2013.

[14] J. Zhu, J. Yang, Z.-F. Bian et al., "Nanocrystalline anatase TiO_2 photocatalysts prepared via a facile low temperature non-hydrolytic sol-gel reaction of $TiCl_4$ and benzyl alcohol," *Applied Catalysis B: Environmental*, vol. 76, no. 1-2, pp. 82–91, 2007.

[15] Q.-H. Zhang, L. Gao, and J.-K. Guo, "Preparation and characterization of nanosized TiO_2 powders from aqueous $TiCl_4$ solution," *Nanostructured Materials*, vol. 11, no. 8, pp. 1293–1300, 1999.

[16] A. Di Paola, M. Bellardita, and L. Palmisano, "Brookite, the least known TiO_2 photocatalyst," *Catalysts*, vol. 3, no. 1, pp. 36–73, 2013.

[17] G. Li and K. A. Gray, "Preparation of mixed-phase titanium dioxide nanocomposites via solvothermal processing," *Chemistry of Materials*, vol. 19, no. 5, pp. 1143–1146, 2007.

[18] K. Yanagisawa and J. Ovenstone, "Crystallization of anatase from amorphous titania using the hydrothermal technique: effects of starting material and temperature," *Journal of Physical Chemistry B*, vol. 103, no. 37, pp. 7781–7787, 1999.

[19] Z. Wang, D. Xia, G. Chen, T. Yang, and Y. Chen, "The effects of different acids on the preparation of TiO_2 nanostructure in liquid media at low temperature," *Materials Chemistry and Physics*, vol. 111, no. 2-3, pp. 313–316, 2008.

[20] B. Gilbert, H. Zhang, F. Huang, M. P. Finnegan, G. A. Waychunas, and J. F. Banfield, "Special phase transformation and crystal growth pathways observed in nanoparticles," *Geochemical Transactions*, vol. 4, pp. 20–27, 2003.

[21] A. Pottier, C. Chanéac, E. Tronc, L. Mazerolles, and J.-P. Jolivet, "Synthesis of brookite TiO_2 nanoparticles by thermolysis of $TiCl_4$ in strongly acidic aqueous media," *Journal of Materials Chemistry*, vol. 11, no. 4, pp. 1116–1121, 2001.

[22] J. Wu, S. Lo, K. Song et al., "Growth of rutile TiO_2 nanorods on anatase TiO_2 thin films on Si-based substrates," *Journal of Materials Research*, vol. 26, no. 13, pp. 1646–1652, 2011.

[23] B. Liu and E. S. Aydil, "Growth of oriented single-crystalline rutile TiO_2 nanorods on transparent conducting substrates for dye-sensitized solar cells," *Journal of the American Chemical Society*, vol. 131, no. 11, pp. 3985–3990, 2009.

[24] A. S. Barnard, P. Zapol, and L. A. Curtiss, "Modeling the morphology and phase stability of TiO_2 nanocrystals in water," *Journal of Chemical Theory and Computation*, vol. 1, no. 1, pp. 107–116, 2005.

[25] A. S. Barnard and P. Zapol, "Effects of particle morphology and surface hydrogenation on the phase stability of TiO_2," *Physical Review B*, vol. 70, no. 23, Article ID 235403, 2004.